ELSEVIER

Ceramics International 30 (2004) 1357–1360

CERAMICS INTERNATIONAL

www.elsevier.com/locate/ceramint

Chemical solution deposition of conductive $SrRuO_3$ thin film on Si substrate

Hisao Suzuki [a,*], Yuki Miwa [a], Hidetoshi Miyazaki [b], Minoru Takahashi [c], Toshitaka Ota [c]

[a] *Department of Materials Science, Shizuoka University, 3-5-1 Jouhoku, Hamamatsu, Shizuoka 432-8561, Japan*
[b] *Institute for Materials Research, Tohoku University, 2-1-1 Katahira, Aoba-ku, Sendai, Miyagi 980-8577, Japan*
[c] *Ceramic Research Laboratory, Nagoya Institute of Technology, 10-6-29 Asahigaoka, Tajimi, Gifu 507-0071, Japan*

Received 1 December 2003; received in revised form 10 December 2003; accepted 22 December 2003

Available online 31 July 2004

Abstract

The conductive metal oxide of $SrRuO_3$ (SRO) thin films were deposited on Si(1 0 0) substrate by spin-coating with a chemical solution deposition (CSD). A stable precursor solution could be prepared from $RuCl_3{\cdot}2H_2O$ as a Ru source and Sr or $SrCl_2$ as a Sr source in 2-methoxyethanol. Highly (2 0 0)-oriented SRO films with a perovskite structure were obtained by the annealing at above 600 °C. As a result, relatively good SRO thin films could be deposited from a precursor solution of Sr and $RuCl_3{\cdot}2H_2O$ by annealing at 700 °C, showing a low resistivity of $1.1 \times 10^{-3}\ \Omega$ cm.

Keywords: D. Perovskite; Chemical solution deposition; $SrRuO_3$; Oxide electrode; Thin film

1. Introduction

Ferroelectric thin films of $Pb(Zr_xTi_{1-x})O_3$ (PZT) have attracted much attention for their wide applications for memories and MEMS. Previous reports have indicated that the use of a metal electrode resulted in the serious fatigue of the PZT thin films at a relatively short number of switching cycles [1–3]. The origins and mechanisms of fatigue are still controversial. On the contrary, conductive metal oxide such as $SrRuO_3$ (SRO) [4–7], $YBa_2Cu_3O_{7-x}$ [8,9], IrO_2 [10], RuO_2 [11], $LaNiO_3$ (LNO) [12], and $La_{0.5}Sr_{0.5}CoO_3$ (LSCO) [13,14] were found to be the effective candidates to improve the fatigue property for PZT thin film capacitors. All these materials show electrical resistivities of a few hundred μΩ cm. In addition, the selection of an electrode material will determine the microstructure and the properties of ferroelectric thin films. The deposition of the lattice-matched heterostructures of PZT film capacitors can be expected to improve the electrical properties. Perovskite oxide electrode such as SRO is one of the most promising candidate because of their similar lattice parameters (the lattice parameters for a PZT with a morphotropic phase boundary composition: $a = 4.036$ Å, $c = 4.146$ Å; and the lattice parameters for a SRO with a pseudo-cubic symmetry: $a = 3.93$ Å). Therefore, SRO is mentioned as a candidate of electrode for the PZT thin films, which shows a lattice matching with a PZT and the low resistivity. SRO thin film is mainly prepared by the chemical vapor deposition (CVD), and the SRO thin film by the chemical solution deposition (CSD) have not been reported. CSD from a homogeneous precursor solution can give rise to deposit a thin film with a homogeneous composition and uniform microstructure as well as the preferred orientation if the seeding layer is inserted between the precursor film and the substrate. In addition, processing is easy and the processing temperature is relatively low. In this study, we focused on the preparation and properties of the SRO thin films deposited on Si(1 0 0) substrate with a CSD.

2. Experimental procedure

$RuCl_3{\cdot}2H_2O$ and Sr or $SrCl_2$ as a Sr source were used as raw materials and 2-methoxyethanol was used as a solvent. A stable SRO precursor solution of 0.1 M could be prepared from $RuCl_3{\cdot}2H_2O$ as a Ru source and Sr or $SrCl_2$ as a Sr source in 2-methoxyethanol. The SRO thin films were

* Corresponding author. Tel.: +81-53-478-1157; fax: +81-53-478-1157.
E-mail address: tchsuzu@ipc.shizuoka.ac.jp (H. Suzuki).

0272-8842/$30.00
doi:10.1016/j.ceramint.2003.12.107

deposited on Si(1 0 0) substrate by spin-coating of the precursor solution. The as-deposited thin films were dried at 150 °C for 10 min. to remove residual organics, pre-annealed at 420 °C for 10 min and then finally annealed at temperatures ranging from 500 to 700 °C for 2 h in an electric furnace. The SRO thin films of the thick up to 300 nm were obtained by repeating these operations. The crystalline phases developed in the films were examined by X-ray diffraction (XRD) with Cu Kα radiation. Microstructure of the films was observed by a scanning electron microscope (SEM). Resistivity of the films was measured by a four-point probe resistivity measurement.

3. Results and discussion

3.1. Effect of Sr source on the crystallization and microstructure

SRO precursor solution (0.1 M) could be prepared from $RuCl_3{\cdot}2H_2O$ as a Ru source and Sr or $SrCl_2$ as a Sr source. SRO precursor powders were prepared from different Sr source by drying the precursor solutions gradually at 150 °C in air for 24 h. Fig. 1 shows the results of the thermogravimetry–differential thermal analysis (TG–DTA) for the SRO powders prepared from $SrCl_2$ and $RuCl_3{\cdot}2H_2O$. Fig. 1 shows two steps of weight loss up to 450 °C, whereas the TG curve for SRO precursor powder derived from a metal Sr exhibited one-step weight loss as shown in Fig. 2. Therefore, the SRO precursor powders were heated at 350 or 450 °C in order to investigate the origin of the two step weight loss. The crystalline phases developed in the SRO precursor powder heated at different temperatures were identified by using X-ray diffractometer. The crystalline phases developed in the SRO precursor powder derived from $SrCl_2$ and heat-treated at 350 °C were identified to be $SrCl_2$, RuO_2 and $RuCl_3$, as listed in Table 1. However, the crystalline phases in the SRO precursor powder derived

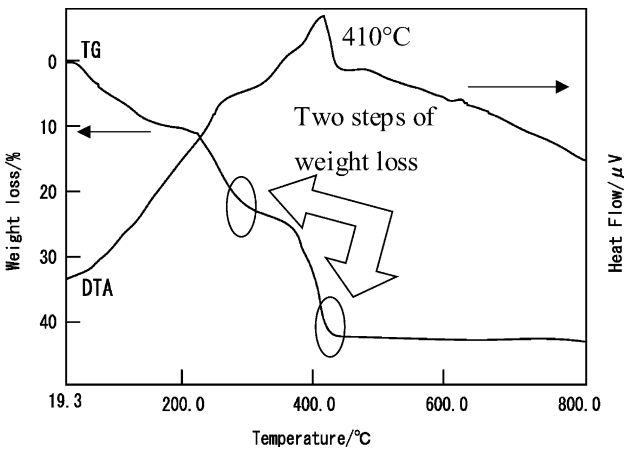

Fig. 1. TG–DTA curves for SRO powder derived from $SrCl_2$ and $RuCl_3{\cdot}2H_2O$.

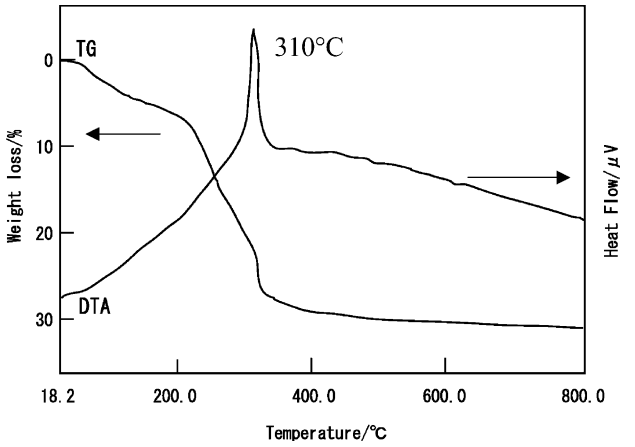

Fig. 2. TG–DTA curves for SRO powder derived from a Sr metal and $RuCl_3{\cdot}2H_2O$.

from a metal Sr and heat-treated at 350 °C were $SrCl_2$ and RuO_2, and the no $RuCl_3$ peak was identified, as shown in Fig. 3. This indicated that the crystallization process was different if the SRO precursor powder was prepared from different Sr source. Moreover, the weight loss for the SRO precursor powders was almost leveled off at above 450 °C. The amount of the weight loss in TG curves is ascribed to the loss of the chlorine from the SRO precursor powders during heating or crystallization as well as the burn out of the residual organics at relatively low temperatures. The only difference in the crystalline phases identified in the SRO precursor powders during annealing was $RuCl_3$ at 350 °C, as shown in Table 1, although the difference in the peak intensity was observed. However, the SRO powders and thin films derived from different precursors were crystallized into a perovskite SRO without any additional phase at above 500 °C, as shown in Fig. 4. From these results, it was concluded that a perovskite SRO powders and films were crystallized by the reaction between $SrCl_2$ and RuO_2 if the precursor was prepared from a metal Sr and $RuCl_3{\cdot}2H_2O$. On the other hand, a perovskite SRO was formed by the reaction among $SrCl_2$, $RuCl_3$ and RuO_2 if the precursor was prepared from a $SrCl_2$ and $RuCl_3{\cdot}2H_2O$. Therefore, the amount of the chlorine burned out during annealing of the thin films at higher temperature should be large if the precursor was prepared from a $SrCl_2$ and $RuCl_3{\cdot}2H_2O$.

For the orientation of the resulting SRO films, all the diffraction peaks can be assigned to a perovskite $SrRuO_3$

Table 1
Crystalline phases developed by the calcination of SRO precursor powders

Annealing temperature (°C)	Sr source	
	$STCl_2$	Sr
250	$SrCl_2$, $RuCl_3$	$RrCl_2$,$RuCl_3$
350	$SrCl_2$, RuO_2, $RuCl_3$	$SrCl_2$, RuO_2
450	RuO_2, $SrCl_2$	RuO_2, $SrCl_2$
>600	Perovskite SRO single phase	

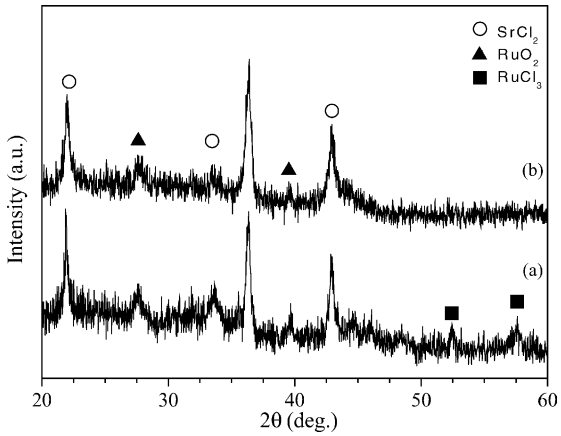

Fig. 3. X-ray diffraction patterns for the SRO powder calcined at 350 °C derived from $SrCl_2 + RuCl_3{\cdot}2H_2O$ (a), and $Sr + RuCl_3{\cdot}2H_2O$ (b), respectively.

with same peaks as those of the 25-0912 JCPDS card. In addition, the as-deposited thin film was SRO single phase and highly (2 0 0)-oriented. Since the all peaks including peak near $2\theta = 32^\circ$ existed and were very similar to those in the SRO thin films deposited by a chemical vapor deposition [4,5,15], SRO films deposited through a CSD in this paper should have the same quality as those of the films deposited by the CVD if the microstructure of the film was same. The peak intensity at around $2\theta = 32^\circ$ for the perovskite SRO films increased with increasing annealing temperature. Therefore, we observed the microstructure of the resulting films by SEM to investigate the relation between film microstructure and the electrical conductivity.

3.2. Electrical conductivity

Electrical conductivity of the thin film is severely affected by the microstructure of the film including the crystallinity, the crystal size, the grain boundary and so on. Therefore,

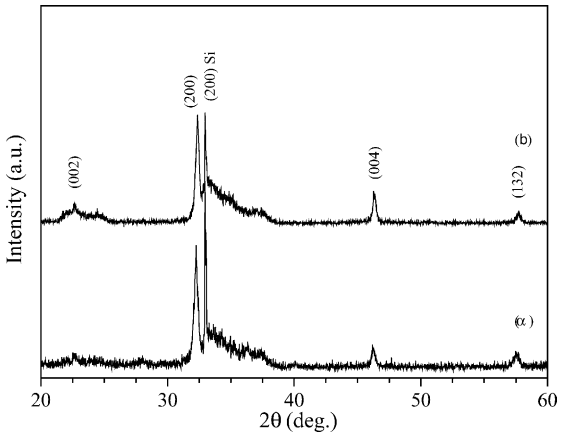

Fig. 4. X-ray diffraction patterns for the SRO thin films annealed at 700 °C derived from $SrCl_2 + RuCl_3{\cdot}2H_2O$ (a), and $Sr + RuCl_3{\cdot}2H_2O$ (b), respectively.

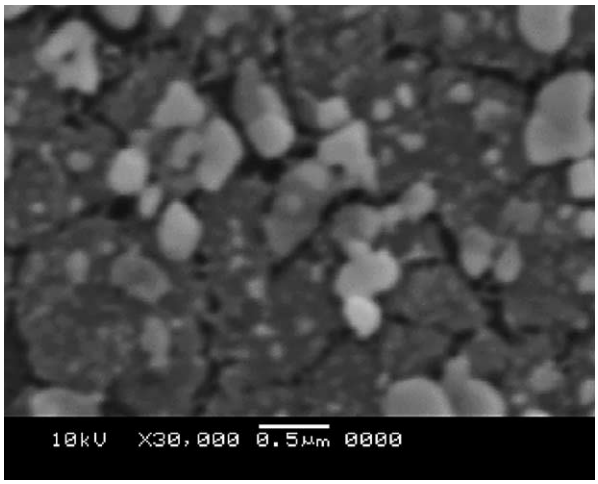

Fig. 5. SEM image of the SRO thin film surface derived from $SrCl_2$ and $RuCl_3{\cdot}2H_2O$ annealed at 700 °C.

the SRO films deposited in this study were observed by the SEM. Figs. 5 and 6 show the surface images of the SRO thin films prepared from $SrCl_2$ and $RuCl_3{\cdot}2H_2O$ or Sr and $RuCl_3{\cdot}2H_2O$, annealed at 700 °C, respectively, because the XRD intensity or the crystallinity of the films increased with increased annealing temperatures and the annealing at higher temperature than this temperature is not good for the semiconductor processing. It is clear that many large pores existed in the SRO thin film prepared from $SrCl_2$ and $RuCl_3{\cdot}2H_2O$ in contrast to the SRO film derived from Sr and $RuCl_3{\cdot}2H_2O$ as shown in Figs. 5 and 6. This result is reasonably explained by the crystallization process of a perovskite SRO phase as already described above. Namely, the SRO precursor derived from $SrCl_2$ and $RuCl_3{\cdot}2H_2O$ crystallizes into a perovskite phase via reactions among $SrCl_2$, RuO_2 and $RuCl_3$, whereas a perovskite SRO formed by the reaction between $SrCl_2$ and RuO_2 in the case of the precursor from Sr and $RuCl_3{\cdot}2H_2O$. This difference of the crystallization into a perovskite phase will give rise to a difference

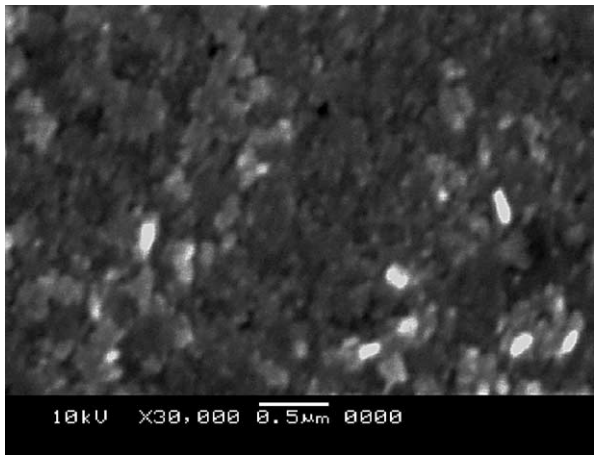

Fig. 6. SEM image of the SRO thin film surface derived from a Sr metal and $RuCl_3{\cdot}2H_2O$ annealed at 700 °C.

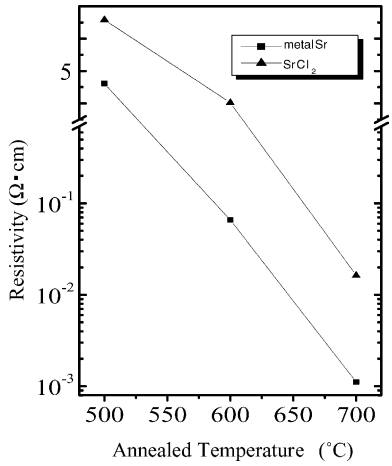

Fig. 7. Resistivity for the SRO thin films annealed at different temperatures.

in the amount of chlorine arose during the annealing, leading to the numbers and the size of the residual pores in the resulting films.

From the above consideration, electrical conductivity should be affected from the difference in the raw materials for precursors and the annealing temperatures because of the difference in the microstructures of the resultant perovskite SRO films. Then, the electrical conductivity or the resistivity of the SRO thin films derived from different raw materials is shown in Fig. 7. The figure shows that the resistivity of the SRO thin films exhibited lower values with increasing annealing temperatures. In addition, resistivity for the SRO thin film from $SrCl_2$ and $RuCl_3{\cdot}2H_2O$ showed higher values compared with those for the SRO thin film from a metal Sr and $RuCl_3{\cdot}2H_2O$, independent of the annealing temperature. The resistivity for the SRO films from $SrCl_2$ and $RuCl_3{\cdot}2H_2O$ and from a metal Sr and $RuCl_3{\cdot}2H_2O$, annealed at 700 °C were 2×10^{-2} and $1 \times 10^{-3}\,\Omega\,\mathrm{cm}$, respectively. The value of $1 \times 10^{-3}\,\Omega\,\mathrm{cm}$ for the SRO film from a metal Sr and $RuCl_3{\cdot}2H_2O$ is very similar to that reported in the previous paper [16], because the relatively dense SRO film was deposited even through the wet chemical processing if the precursor was prepared from appropriate reagents. Therefore, it is concluded that the conductive SRO thin film is successfully deposited with a CSD, which can be used as a electrode for the ferroelectric thin film capacitor structures on the Si wafer.

4. Conclusions

A single-phase SRO thin films were successfully deposited on a Si(1 0 0) substrate by a spin-coating with a CSD from strontium and ruthenium chlorides. The thin films deposited on a Si(1 0 0) substrate were strongly (2 0 0)-oriented, which was suitable for a oxide electrode for a ferroelectric thin film capacitor. The resultant perovskite SRO thin films exhibited different electrical conductivity, depending upon a film microstructures. The difference in the microstructure was ascribed to the crystallization process or row materials for the precursors. As a result, relatively good SRO film could be deposited from precursor solution of Sr and $RuCl_3{\cdot}2H_2O$ by annealing at 700 °C, showing the resistivity of $1 \times 10^{-3}\,\Omega\,\mathrm{m}$.

References

[1] S.Y. Chen, C.L. Sun, J. Appl. Phys. 90 (2001) 2970–2974.
[2] T. Mihara, H. Watanabe, C.A.P. Araujo, Jpn. J. Appl. Phys. 33 (1994) 5281–5286.
[3] H.M. Duiker, P.D. Beale, J.F. Scott, C.A.P. Araujo, B.M. Melnick, J.D. Cuchiaro, L.D. McMillian, J. Appl. Phys. 68 (1990) 5783–5791.
[4] K. Aoki, I. Murayama, Y. Fukuda, A. Nishimura, Jpn. J. Appl. Phys. 36 (1997) L690–L692.
[5] Y.K. Wang, T.Y. Tseng, P. Lin, Appl. Phys. Lett. 80 (2002) 3790–3792.
[6] T. Morimoto, O. Hidaka, K. Yamakawa, O. Arisumi, H. Kanaya, T. Iwamoto, Y. Kumura, I. Kunishima, S. Tanaka, Jpn. J. Appl. Phys. 39 (2000) 2110–2113.
[7] C. Guerrero, J. Roldan, C. Ferrater, M.V. Garcia-Cuenca, F. Sanchez, M. Varela, Solid State Electron. 45 (2001) 1433–1440.
[8] R. Ramesh, W.K. Chan, B. Wilkens, H. Gilchrist, T. Sands, J.M. Tarascon, V.G. Keramidas, D.K. Fork, J. Lee, A. Safari, Appl. Phys. Lett. 61 (1992) 1537–1539.
[9] J. Lee, L. Johnson, A. Safari, R. Ramesh, T. Sands, H. Gilchrist, V.G. Keramidas, Appl. Phys. Lett. 63 (1993) 27–29.
[10] T. Nakamura, Y. Nakao, A. Kamisawa, H. Yakasu, Jpn. J. Appl. Phys. 33 (1994) 5207–5210.
[11] S.D. Bernstein, T.Y. Wong, Y. Kisler, R.W. Tustison, J. Mater. Res. 8 (1993) 12–13.
[12] B.G. Chae, Y.S. Yang, S.H. Lee, M.S. Jang, S.J. Lee, S.H. Kim, W.S. Beak, S.C. Kwon, Thin Solid Films 410 (2002) 107–113.
[13] R. Dat, D.J. Lichtenwalner, O. Auciello, A.I. Kingon, Appl. Phys. Lett. 64 (1994) 2673–2675.
[14] R. Ramesh, H. Gilchrist, T. Sands, V.G. Keramidas, R. Haakenaasen, D.K. Fork, Appl. Phys. Lett. 63 (1993) 3592–3594.
[15] J.P. Mercurio, J.H. Yi, M. Manier, P. Thomas, J. Alloys Compd. 308 (2000) 77–82.
[16] J. Roldan, F. Sanchez, V. Trtik, C. Guerrero, F. Benitez, C. Ferrater, M. Varela, Appl. Surf. Sci. 154 (2000) 159–164.